P2.35 Numerical Accuracy of the Regional Spectral Method used in NCEP RSM

*Jun Wang and Hann-Ming Henry Juang**

Environmental Modeling Center, NCEP, Washing, DC

1. INTRODUCTION

In 1986, Tatsumi developed a spectral limited area model with time-dependent lateral boundary conditions using an orthogonal double Fourier series. Since then more regional spectral models have been developed (Wang 2004). Hoyer (1987), Fulton and Schubert (1987) , Machenhauer (1993), Chen and Kuo (1992) and Juang and Kanamitsu (1994) all independently developed their own regional spectral models. These regional spectral models have been used to simulate and to predict regional climates due to the capability of resolving regional variation more accurately (Hong et and Leetmaa 1999, Cocke and Larow 2000).

Lateral boundary treatment is one of very important elements in regional spectral models to blend the global field into regional domain.(Baumhefner 1982, Laprise 2002, Boyd 2004). Tatsumi (1986) used time dependent lateral boundary conditions as mentioned before. Machenhauer (1986), Haugen and Machenhauer (1993) used cyclic boundary conditions with an artificial extended domain. In 1992, when Kuo and Williams presented results on the boundary effects in regional spectral models, they concluded that due to the discontinuity of higher derivatives of the sinusoidal subtracted sine-cosine expansion in the Tatsumi method, this expansion causes the Gibbs phenomenon. Furthermore, in 1998 they discussed the scale dependent accuracy of the regional spectral method and claimed that the large scale spatial accuracy is worse than the small scale spatial accuracy. Here we present the Numerical methods used in NCEP RSM (National Centers for Environmental Prediction Regional Spectral Model), examine its numerical accuracy and scale dependency, and compare the results between NCEP RSM and Tatsumi's method in Kuo and Williams's paper. From here on, Kuo and Williams (1992 and 1998) will be referred as KW92 and KW98, respectively.

A simple linear advection equation used in Kuo and Williams (1992, 1998) is adopted to explore the numerical accuracy of the NCEP RSM method. Section 2 gives the numerical method used in NCEP RSM. Section 3 addresses the experimental design, including the model problem and numerical schemes. Results are shown in Section 4. In Section 5 some sensitivity tests are conducted to discuss the effects to the accuracy from the time step, spatial resolution for both regional and background domains, and the time scheme and interpolation methods. Conclusions are made in Section 6.

2. Regional Spectral Method in NCEP RSM

In NCEP RSM, the full-field prognostic variable is divided into a base field and perturbation field, which is different from Tatusmi's (see Fig. 1 of Juang et al. 1997).

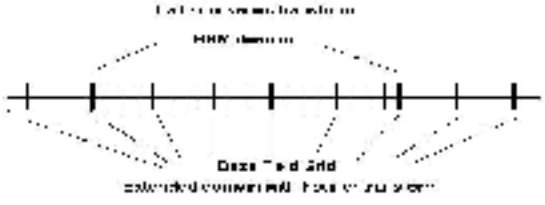

Fig. 1 The NCEP RSM method grid system.

* Corresponding author address: Dr. Hann-Ming Henry Juang, NOAA National Sciences Center, Room 207, 5200 Auth Road, Camp Springs, MD 20746. Email address: henry.juang@noaa.gov

An alternative description, supplemented to previous publications on the NCEP RSM, is illustrated by Fig. 1. The full-field variable A, for example, is separated into two parts, the base field $\overline{A}$ and perturbation A' as:

$$A = \overline{A} + A' \qquad (2.1)$$

The base field can represent a trend and the perturbation can be performed Fourier transformation (Laprise 2003). For the integration, the perturbation field is obtained by updating the deviation of the regional total tendency from the base field tendency on the regional domain:

$$\frac{dA'}{dt} = \frac{dA}{dt} - \frac{d\overline{A}}{dt} \qquad (2.2)$$

The perturbation tendency is computed in each time step, and then the perturbation filed is used to form the total field. When the perturbation is updated, spectral truncation is conducted in order to maintain the perturbation field smooth in the integration domain.

3. Experiment Design

3.1 Numerical problems

The numerical problem used here is the same one-dimensional linear advection equation shown in KW 92:

$$\frac{\partial A}{\partial t} + u_0 \frac{\partial A}{\partial x} = 0 \qquad (3.1a)$$

where A is any given variable, t is time and x is a spatial variable in the domain [-1,1], and u_0 is a constant speed of 1 m/sec. Considering scale variation, we use the initial condition from KW98:

$$A(x, t=0) = \exp\left[-\left(\frac{x+0.5}{L}\right)^2\right] \qquad (3.1b)$$

the boundary condition is:

$$A(-1, t) = g(t) = \exp\left[-\left(\frac{-0.5-u_0 t}{L}\right)^2\right], \qquad (3.1c)$$

and the analytical solution of this problem is:

$$A_{ana}(x,t) = \exp\left[-\left(\frac{x+0.5-u_0 t}{L}\right)^2\right] \qquad (3.2)$$

This simple model describes an advection processes involving a wave propagating into the regional domain from left to right. The boundary effect will be seen when the wave passes through the right boundary at x=1. L is the spatial-scale parameter that determines the wave scale in the domain. The changes in L will show the scale dependent accuracy in the numerical solutions.

3.2 Numerical methods

The fourth order finite-difference method (FD4) and the sixth order finite-difference method (FD6) are implemented for comparison. Since the NCEP RSM method uses a leapfrog time scheme, which is also used for both the fourth order finite-difference method and the sixth order finite-difference method.

Applying NCEP RSM method, we get the integration equation as:

$$\frac{A_j'^{n+1} - A_j'^{n-1}}{2\Delta t} = -\left(\frac{\partial \overline{A}}{\partial x}\right)^n - \left(\frac{\partial A'}{\partial x}\right)^n - \frac{\Delta \overline{A}}{\Delta t} \qquad (3.3)$$

Initially, A is the analysis solution located on the regional fine grid and the analysis solution on the coarse grids. The coarse grid is extended to a large domain so that enough information around the regional lateral boundary can be obtained. This is the fundamental difference between NCEP RSM and Tatusmi's method. Since the base field has more information, the spatial derivative of the base field is closer to real value. It will result in better perturbation field than that in Tatusmi's method. To solve the numerical problem (3.1), we obtain the base field on the regional fine grid by extending the coarse grid base field into the Fourier series, and then conducting the inverse Fourier transform to a fine grid over the coarse domain. The initial perturbation is obtained by subtracting the base field from the analysis solution in the regional domain. The tendency of the base field on RHS is calculated with large time intervals using a leap frog time scheme. This tendency is also used to update the base field at every regional time step. The spatial derivative of the base field $\frac{\partial \overline{A}}{\partial x}$ is calculated from a spectral transform through the Fourier series coefficients of the aforementioned base field. The spatial derivative of the

perturbation field $\frac{\partial A'}{\partial x}$ is calculated through the half sine-wave series coefficients of the perturbation field. After the perturbation field is updated through Eq. (3.6) at every time step, a sine-wave truncation is conducted to make sure that the perturbation field spectrum is filtered without introducing Gibbs waves due to discontinuities. No lateral boundary relaxation is applied to this problem.

4. Results

4.1 A comparison with the results of KW92

Figure 2 shows the numerical solution from the NCEP RSM method and FD4 method for Eqs. (3.1a-3.1c) when L=0.2, N=24 and the time step=0.01 at t=1.0 and 1.5. The results from RSM keep the wave structure very well when the wave passes the right boundary. Compared to Fig. 1 in KW92, the results from NCEP RSM show significant difference from he polynomial-subtracted method (PST) and sinusoidal-subtracted method (SST) method, and no Gibbs phenomenon shows up in either the incoming or outgoing boundary regions.

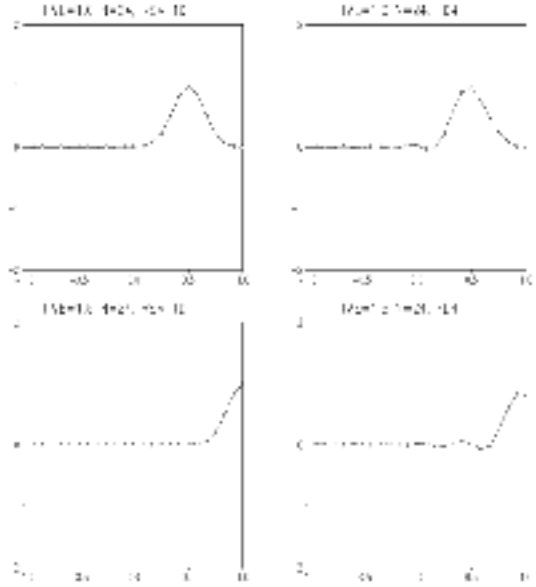

Fig. 2 Numerical solutions from the NCEP RSM method and from FD4 for Eqs.(3.1a) - (3.1c) with N=24 at t=1.0 and1.5, and time-step=0.01.

4.2 A comparison with the results of KW98

RMSEs in the numerical solutions as a function of regional grid number N and spatial scale parameter L are shown in Fig. 3. The left panel is for FD4 and right one is for the NCEP RSM method. Fig. 3 shows that the RMSEs from the NCEP RSM numerical solution are smaller than FD4. What it does not show is what is seen in Fig. 2 in KW98, where the RMSE increases with a large spatial scale parameter L greater than 0.2; instead, RMSE decreases when the scale parameter L increases. In the left panel the FD4 slope is sharper than that of the NCEP RSM method, and the RMSE increases from less than to greater than for N greater then 64 when the space scale L is greater than 0.3. This means that the scale dependence accuracy problem does not exist in NCEP RSM method.

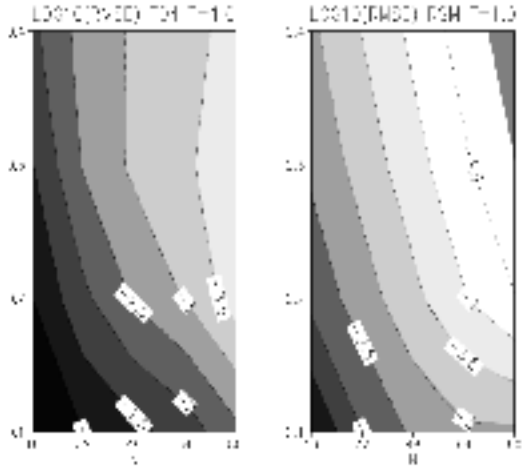

Fig. 3 RMSE (in log10 form) in the numerical solutions of FD4 (left panel) and NCEP RSM (right panel) as a function of L and N at t=1.0.

5. Sensitivity test

5.1 Temporal and spatial resolutions and Scheme comparison

In this paper, the effects of temporal and spatial resolutions to the integration are explored. For fixed regional grid points N with the time step decreasing, when the wave passes the left and right boundaries, the RMSE decreases NCEP RSM. The NCEP RSM method always keeps the widest range and has the best solution when the time steps get smaller. the 4th order finite-difference method and the spectral transform are used to compute the base field spatial derivative. The results show better accuracy from the base field tendency, therefore, this method produces much better results. Two time schemes, a central difference time scheme (CDTS) and

a temporal spectral scheme (TSPEC), are used to calculate the base field tendency. The TSPEC produces a better solution at large time steps and it changes less when the time step increases since the same time series are provided for the different time resolutions.

5.2 Base field resolution

As we have seen, how to introduce the base field is essential for regional spectral methods. In the NCEP RSM method, the base field in the regional domain is interpolated from the global domain through the spectral method. Practically, the global domain is bigger than whole regional domain. For the model problem (3.1) the base field domain is chosen to be 4 times as big as the regional domain. If N_g is the

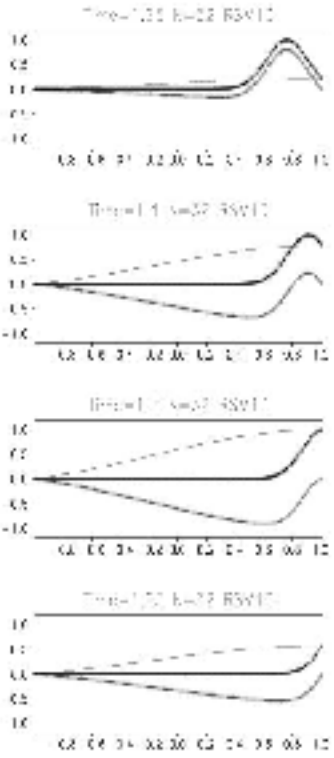

Fig.4 Numerical solution from the NCEP RSM method when Ng=1 and N=32. The dotted line is the numerical solution u, the solid line is the spectral interpolated base field, and the plus sign line is the perturbation field.

number of coarse grid points in the regional domain, N is the number of regional grid points. The results show that when N_g is increasing, the RMSE is correspondingly decreasing. When N_g =16 enough information is provided for the NCEP RSM method to produce a minimum error solution. The errors do not change when larger enough N_g is provided.

Fig4 shows the numerical solution when t=1.25, 1.4, 1.5, and 1.65 when N_g =1, N=32 and =. The base fields are only provided at both boundaries in the regional domain and they are also located in five grid points in the extended base field domain as shown in Figure 1. From the figure, changes or time variation at the right boundary is captured by the base field, where the base field shows a smooth line with increasing slope at t=1.25, t=1.4 and t=1.5, then the slope goes down at t=1.65. At the same time, the perturbation field that contains most of the information about the total solution conducts a corresponding change. At t=1.25, the perturbation is much like the total field since the base field is almost zero; then the perturbation field is adjusted to recover the total domain at the inner domain and maintain a zero condition at the right boundary. The results shows how the perturbation field recovers the total field even it has potential exponential convergence problem due to use of Fourier Series.

6. Conclusion

The same one dimensional advection problem used in KW92 and KW98 has been employed in this paper to discuss the boundary effects and scale dependent accuracy in the NCEP RSM method. The results show that the solution does not have the Gibbs Phenomenon when a wave passes through both incoming and outgoing the boundaries. The NCEP RSM method doesn't have an error jump as shown in 4th and 6th order finite difference methods and SST/PST methods in KW92 and KW98. The different choice of base field explains the difference. Specifically, a base field provided at both boundaries in the regional domain and also located in five grid points in the extended base field domain are used to show how the perturbation field could recover the total field.

Sensitivity tests have been conducted to investigate the effects on the numerical solution from some factors such as base

field selection, boundary conditions, interpolation method, difference methods and time scheme. When computing a base field spatial derivative, the spectral method gives a smaller error than the finite difference method because the error from the finite difference method will dominate the total error. And the temporal spectral method derives a better solution than the central differencing time scheme.

References

Baumhefner, D. P., and D. J. Perkey, 1982: Evaluation of lateral boundary errors in limited domain model. Tellus, 34, 409-428

Boyd, J. 2005: Limited_area Fourier Spectral Models and data analysis schemes: Windows, Fourier Extension, Davies Relaxation, and all that. Mon. Wea. Rev. 133, 2030-2042.

Chen, Q.-S., and Y.-H. Kuo, 1992: A harmonic-sine series expansion and its application for partitioning and reconstruction problems in a limited area. Mon. Wea. Rev., 120, 91-112

Cocke, S., and T.E. Larow, 2000: Seasonal Predictions using a Regional Spectral model Embedded within a Coupled Ocean-Atmospheric Model. Mon. Wea. Rev., 128, 689-708

Fulton, S.R. and W.H. Schubert, 1987a: Chebyshev spectral methods for limited area models. Part I: model problem analysis. Mon. Wea. Rev., 115, 1940-1953

------, and -----, 1987b: Chebyshev spectral methods for limited area models. Part II: shallow water model. Mon. Wea. Rev., 115, 1954-1965

Haugen, J.E., and B. Machenhauer, 1993: A spectral limited-area model formulation with time dependent boundary conditions applied to the shallow water equations. Mon. Wea. Rev., 121, 2618-2630

Hoyer, J.M., 1987: The ECMWF spectral limited-area model. Proc. ECMWF Workshop on Techniques for Horizontal Discretization in Numerical Weather Prediction Models, Berkshire, Reading, United Kingdom, ECMWF, 343-359

Hong S.Y., and A. Leetmma 1999: An Evaluation of the NCEP RSM fir regional climate modeling. J. Climate, 12, 592-609

Juang, H.M. and M. Kanamitsu, 1994: The NMC nested regional spectral model. Mon. Wea. Rev., 122, 3-26

----- , S.Y. Hong, and M. Kanamitsu, 1997: The NCEP regional spectral model: An update. Bull. Amer. Meteor. Soc., 78, 2125-2143

------, and S.Y. Hong, 2001: Sensitivity of the NCEP regional spectral model to domain size and nesting strategy, Mon. Wea. Rev., 129, 2904-2922

Kanamistu, M., K. Tada, T. Kudo, N. Sato, and S. Isa, 1983: Description of the JMA operational spectral model. J. Meteor. Soc. Japan, 61, 812-828.

Kuo, H,C, and R.T. Williams, 1992: Boundary effects in regional spectral models. Mon. Wea. Rev. 120,2986-2992

Kuo, H,C, and R.T. Williams, 1998: Scale-dependent accuracy in regional spectral model. Mon. Wea. Rev. 126, 2640-2647

Elia R., R. Laprise and R. Denis, 2006: Forecasting skill limits of Nested_area models: a perfect approach, Mon. Wea. Rev. 130, 2006-2023

Laprise, R., 2003: Resolved scales and nonlinear interactions in limited-area models. J. Atmos Sci, 60, 768-779

Machenhauer, B., 1986: Limited-area modeling by the HIRLAM preject group, Preprints, HIRLAM, No. 1, 13pp

Tatsumi, Yi, 1986: A spectral limited-area model with time dependent lateral boundary conditions and its application to a multi-level primitive equation model. J. Meteor. Soc. Japan, 64, 637-663

Wang,Y., L. Leung, J. McGregor, D. Lee, W. Wang, Y. Ding and F. Kimura, 2004: J. Meteor. Soc. Japan, 82,1599-1628